Automation in Construction 113 (2020) 103161

Contents lists available at ScienceDirect

Automation in Construction

journal homepage: www.elsevier.com/locate/autcon

Feasibility study of lego-inspired construction with bendable concrete

Yi Bao[a,b], Victor C. Li[b,*]

[a] Department of Civil, Environmental and Ocean Engineering, Stevens Institute of Technology, Hoboken, NJ 07030, USA
[b] Department of Civil and Environmental Engineering, University of Michigan, Ann Arbor, MI 48109, USA

ARTICLE INFO

Keywords:
Automation in construction
Bendable concrete
Dry joints
Lego-inspired construction
Precast
Reconfiguration

ABSTRACT

Current construction of engineering structures faces a variety of challenges, such as shortage of skilled labor, low adaptation to new technologies, and increasing concerns for negative impacts on the environment. These challenges have significantly compromised the productivity and economic benefits of the construction industry. Further, construction activities have been linked to significant emissions, particularly CO_2 associated with global warming. This study proposes a new paradigm of construction – Lego-inspired construction, and investigates the feasibility. Inspired by Lego blocks that can be assembled via dry joints and disassembled for different objects, this study presents blocks made using a bendable concrete, aiming to assemble various structures with dry joints. The blocks are used to assemble a prototype footbridge to demonstrate the assembling process, which is compatible with robotic systems for construction automation. The footbridge demonstrated reasonable load-carrying capability in mechanical testing. After the testing, the footbridge was disassembled, and the blocks were reused to assemble a frame for buildings. The proposed Lego-inspired construction is promising to greatly improve the construction efficiency and reduce the adverse impacts on the natural environment caused by conventional construction approaches.

1. Introduction

In the U.S., labor productivity in construction declined by > 50% from 1968 to 2010, according to McKinsey Global Institute 2017 Report on construction [1]. That is consistent with the worldwide trend of declining productivity in construction. The U.S. and multiple developed countries have been classified as “declining leaders”, which are featured with negative construction productivity growth while retaining high overall productivity [1]. The lagging construction productivity annually costs about 0.6 trillion dollars for the economy of the U.S., and 1.6 trillion dollars for the global economy [1]. The low productivity results from a variety of challenges, such as shortage of skilled labor willing to work on construction sites [2], low adaptation to new technologies [3], and increasing concerns for negative impacts of construction activities on the natural environment [4]. While emerging technologies such as digital manufacturing have been utilized in many industries to radically modernize the processes, construction remains one of the most stagnant industries that use the same methods developed a century ago. While construction is full of highly repeatable processes, the majority of construction projects are still treated as one-off prototypes and start from scratch manually, thus sacrificing time and cost efficiencies.

In concrete construction, there are two main approaches: cast-in-place and precast. In general, the precast approach is more efficient than the cast-in-place approach, which has restricted casting sequence that limits the construction efficiency. For instance, in a bridge construction, the piers must be cast and gain sufficient mechanical strength, before the girders can be cast. In precast construction, different structural components can be fabricated offsite and in parallel, and rapidly installed in the field. Precast construction has shown great success in accelerated bridge construction [5–7] and modular construction for the housing market [8,9], both improving the construction productivity, safety, and economic and environmental benefits, due to the use of prefabricated components.

Despite the success, the current precast construction practices face limitations. (1) The designs of structures limit the construction efficiency. Currently, most prefabricated elements are connected using wet joints (fresh grouts), which need time to cure [10]. In the context of transportation infrastructure, such as bridges, the limited construction efficiency increases the downtime and aggravates traffic congestion, compromising the mobility, economic benefits, and quality of life. Traffic delay costs billions of dollars in wasted gas and person hours per year, without considering the adverse effects on the environment and human health. (2) Current structures cannot be reused, generating a

* Corresponding author.
E-mail address: vcli@umich.edu (V.C. Li).

https://doi.org/10.1016/j.autcon.2020.103161
Received 24 September 2019; Received in revised form 28 February 2020; Accepted 28 February 2020

large amount of construction and demolishment (C&D) wastes. Although concrete may be recycled, the recycling process involves multiple treatment stages such as sorting, crushing, and cleaning, thus increasing the cost. In practice, recycled concrete is used as a lower grade concrete compared with normal concrete. The recycling rate of C&D wastes is limited. While roads and bridges annually produce > 150 million tons of concrete waste in the U.S. [11], < 40% is recycled. The remaining portion is disposed through landfill, but the area available for landfill is shrinking. (3) The structures are less aesthetically attractive. For instance, modular construction delivers stereotyped bulky boxes. (4) High demand of skilled labor and low adoption of robotic systems limit the construction productivity. The majority of precast structures uses unique prefabricated elements that are not exchangeable among different structures, and the construction process can hardly be standardized and realized using construction robots.

The above problems are exacerbated by the aging structures. According to ASCE 2017 Report Card [12], the condition of roads was rated “D”, and the condition of bridges was rated “C+”. According to U.S. Department of Transportation [13], < 50% of the bridges in the U.S. are rated “good”; 25% of publicly owned bridges are structurally deficient or functionally obsolete. Thus, approximately 150,000 bridges need to be rebuilt or rehabilitated. There is an urgent need of innovative solutions that improve construction efficiency, mobility, resilience, and sustainability.

This study presents a new paradigm of construction – Lego-inspired construction. Lego blocks are popular toys that kids use to assemble various structures such as bridges and buildings. Limited types of standard blocks are manufactured for general applications. This can be supplemented with special blocks for specific projects. In all cases, the blocks are manufactured for assembling structures through dry joints, which can be disconnected without damaging the blocks. The user can reuse the blocks to assemble a structure with a totally different configuration, as depicted in Fig. 1. Following this concept, it is envisioned that a variety of structures can be assembled using large scale blocks that can be prefabricated offsite and assembled in the field via dry joints, which can be disconnected for reconfiguration. It is further postulated that assembling and disassembling operations can be performed using robotic systems.

This study aims to demonstrate the feasibility of Lego-inspired construction, and validate the load-carrying capability of a prototype footbridge assembled using Lego-inspired blocks. The rest of the paper is organized as follows. Section 2 introduces designs of Lego-inspired blocks made using a bendable concrete. Section 3 reports the assembly process and laboratory testing of the bridge. Section 4 demonstrates the reconfigurability of the bridge. Based on the investigations in Sections 2 to 4, Section 5 discusses important features of the Lego-inspired construction. Section 6 delivers the conclusions.

2. Lego-inspired blocks

This section introduces the material and design of the blocks for Lego-inspired construction. To resist various loads during construction and operation of structures, a bendable concrete is used to fabricate the blocks. Preliminary designs of blocks are presented based on the bendable concrete. Bendable concrete was chosen as the preferred material for the blocks due to its damage tolerant behavior under concentrated loads, making the resulting blocks jointable by steel nuts and bolts without suffering from brittle fracture. These bendable concrete blocks are trade-named RecoBlox™.

2.1. Bendable concrete

The bendable concrete, also known as Engineered Cementitious Composites (ECC), was developed in a previous research [14]. The mixture was prepared using ASTM Type I Portland cement, Class F fly ash, finely ground quartz sand, polyvinyl alcohol (PVA) fibers, and tap water. The quartz sand had an average diameter of 75 μm and a density of 2.63 g/cm^3. The PVA fibers were 8 mm in length, 39 μm in diameter, and 1300 kg/m^3 in density; the tensile strength, Young's modulus, and ultimate elongation of the PVA fibers were 1.6 GPa, 43GPa and 6%–8%, respectively. In the mixture, the water-to-binder ratio was 0.25; the sand-to-binder ratio was 0.36; the PVA fiber volume percentage was 2% by the volume of the concrete. The binder was composed of 30% cement and 70% fly ash, by mass. A high range water reducer was used at a dosage of 0.1% by volume of the binder to make the mixture self-consolidating.

The mixture was mixed using a 60-Qt. (57-L) Hobart mixer. First, the cement, fly ash, and quartz sand were mixed in dry condition at 60 rpm for 5 min. Then, the high range water reducer was dissolved in water and introduced to the mixer, and mixed at 120 rpm for 5 min. Finally, the PVA fibers were manually added at 60 rpm in 2 min, followed by mixing at 120 rpm for 3 min. On completion of mixing, the mixture was checked by hand, and no fiber agglomeration was found.

The compressive strength was determined using 50-mm cubes in accordance with ASTM C 109 [15]. Three samples are replicated in each test. The loading rate was maintained at 1.8 kN/min until failure. The compressive strength was 46 MPa ± 2 MPa. Four dog-bone specimens (Fig. 2(a)) were tested under tension at a displacement rate of 0.05 mm/min in accordance with [16]. The applied load and specimen elongation within the 80-mm gauge length were measured using an embedded load cell and two external linear variable differential transformers, respectively. Fig. 2(b) shows a set of tensile stress-strain curves. The mixtures had a tensile strength of 5.8 MPa ± 0.2 MPa and an ultimate strain of 4.6% ± 0.3%.

The bendable concrete is a version of Engineered Cementitious Composite (ECC) featured with high tensile ductility [17–19].

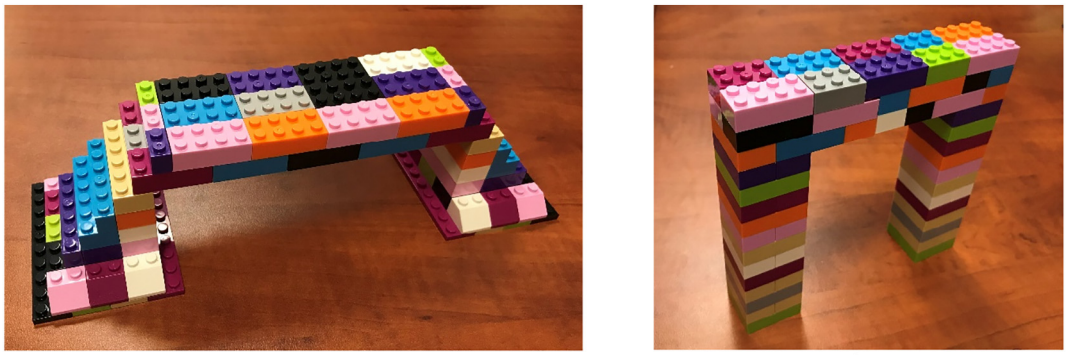

Fig. 1. Depiction of Lego-inspired construction. (a) Lego blocks are used to assemble a footbridge. (b) The same blocks used in the footbridge are reused to assemble a frame for building.

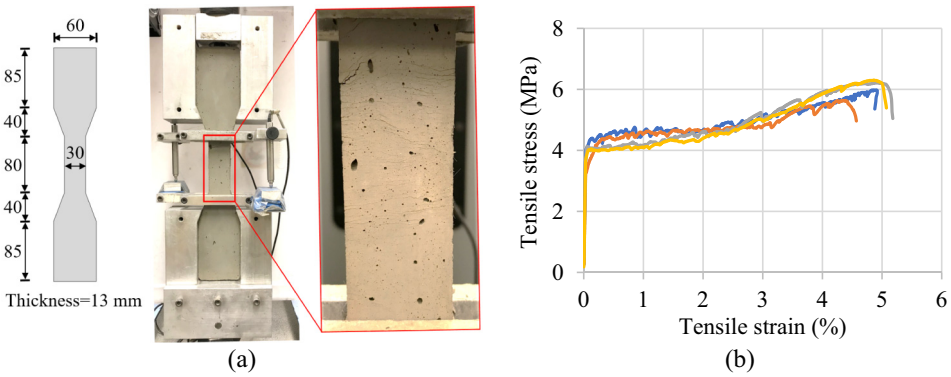

Fig. 2. Tensile test: (a) setup and specimen (unit: mm); (b) stress-strain curves of four specimens.

Typically, the tensile strain corresponding to the peak tensile stress is higher than 4%, which is > 400 times that of conventional concrete. Once cracked, conventional concrete fails to resist tensile force, while ECC maintains resistance to tensile force, as shown in Fig. 2. Compared with fiber-reinforced concrete, ECC exhibits strain-hardening behavior, which means that the tensile stress continues increasing with the tensile strain after initial microcracking [20]. The unique tension resistance of ECC makes it an attractive structural material for resistance to seismic loading [21–23], impact loading [24], and bolting or anchoring force [25].

In addition to the unique tension resistance, ECC has unique crack patterns and durability. Due to the bridging effect of chopped fibers dispersed in ECC matrix, ECC has controlled tight crack widths (~60 μm). The controlled crack width ensures that cracked ECC behaves similar to uncracked ECC, in terms of the transport properties [26]. More interestingly, the tight crack can be self-healed in air with presence of moisture [27]. The healed ECC demonstrated comparable stiffness and permeability with those of intact ECC specimens. The use of PVA fibers in ECC also improved the spalling resistance of ECC at high temperature [28]. Recently, multifunctionality has been imparted into ECC by incorporating functional materials. For instance, carbon black was used to increase the electrical conductivity of ECC and achieve self-sensing function [29]; titanium dioxide nanoparticles were added to ECC to achieve self-cleaning and air-purifying functions [30].

2.2. Lego-inspired blocks

Fig. 3 shows four blocks (RecoBlox™) designed following the criteria informed by the Lego-inspired construction. The main criteria include: (1) the blocks are connected with dry joints that can be disconnected without damaging the blocks; (2) the joints are not the weakest positions that limit the mechanical performance of the blocks; (3) the blocks have reasonable mechanical load resistance; (4) the assembling and disassembling operations can be performed by robotic systems; and (5) the blocks can be prefabricated offsite with high quality. In addition to these requirements, this feasibility study uses blocks suitable for manual operation by a single person. With these considerations, the blocks are designed to be jointed via shear keys and steel bolts.

The four blocks are designated B1, B2, B3, and B4, respectively. Among them, B1 is a full block with a box section; its top and bottom plates are flat, and its side plates (walls) have shear keys and holes for passing the steel bolts. B2 is a half of B1. B3 and B4 are plates, which are the same as the two side plates of B1, respectively. All the blocks have shear keys and holes for passing the steel bolts. This study adopted Grade 5 steel bolts with a tensile strength of 827 MPa. The bolts measured 12.7 mm in nominal diameter and 88.9 mm in length.

3. Demonstration of Lego-inspired construction

3.1. Footbridge design

To demonstrate the performance of the Lego-inspired blocks, the four types of blocks are used to assemble a footbridge, as depicted in Fig. 4. The footbridge is simply supported on rigid supports with a span length of 2.8 m. The footbridge is designed to resist its self-weight and the action of two adults walking through the bridge. Structural analysis of the bridge was performed using finite element models established using the software ABAQUS [31]. The blocks were modeled using eight-node solid elements (C3D8R). The material properties obtained from the material testing were adopted in the finite element model. Surface-to-surface hard contact was defined for each pair of contacted surfaces. Through the influence line analysis, the most undesired loading scenario was determined – applying the pedestrian load at the mid-span of the bridge. According to the finite element analysis, under the combination of self-weight and pedestrian load, the maximum tensile stress in the bridge is 4 MPa, which is close to the first crack strength (see Fig. 2). Considering the concept of Lego-inspired construction, the blocks will be reused after the structure is disassembled. Thus, the structure should be designed to be free of crack under design operation loads. To avoid cracking, post-tensioned bars are used to apply prestressing forces. The magnitude of the prestressing forces in the bars was analyzed and determined using the finite element model to ensure the maximum tensile stress in the blocks is below the first crack stress of the concrete. Although the footbridge is designed to be free of cracking under loading, the use of the bendable concrete is important in ensuring the integrity of the blocks and prevents catastrophic cracking during the assembling process. The damage tolerance of the bendable concrete (see Fig. 2) protects the blocks from damage in the process of applying bolting force at the connection between adjacent blocks.

3.2. Construction process

The construction process of the footbridge was divided into three main steps: (1) assembling the prefabricated blocks, (2) applying prestressing force, and (3) lifting and placing the bridge on supports. Fig. 5 depicts the assembling sequence, as indicated by the numbers marked on the blocks. During assembling, the blocks were laid on a flat surface in the laboratory; adjacent blocks were connected via the shear keys and bolts. The shear keys and bolts were at the side walls of the blocks. For instance, the block No. 7 was directly connected with the blocks 3, 6, 8, and 11 at the side walls. Although the block 7 was in direct contact with the blocks 4 and 10, there was no shear connector and bolt between blocks 4 and 7 or between 7 and 10. Under external loading, there may be compression between each pair of contacting surfaces, such as the surfaces at the interface between blocks 4 and 7. A torque wrench was used to manually apply a consistent torque (55 N·m) to

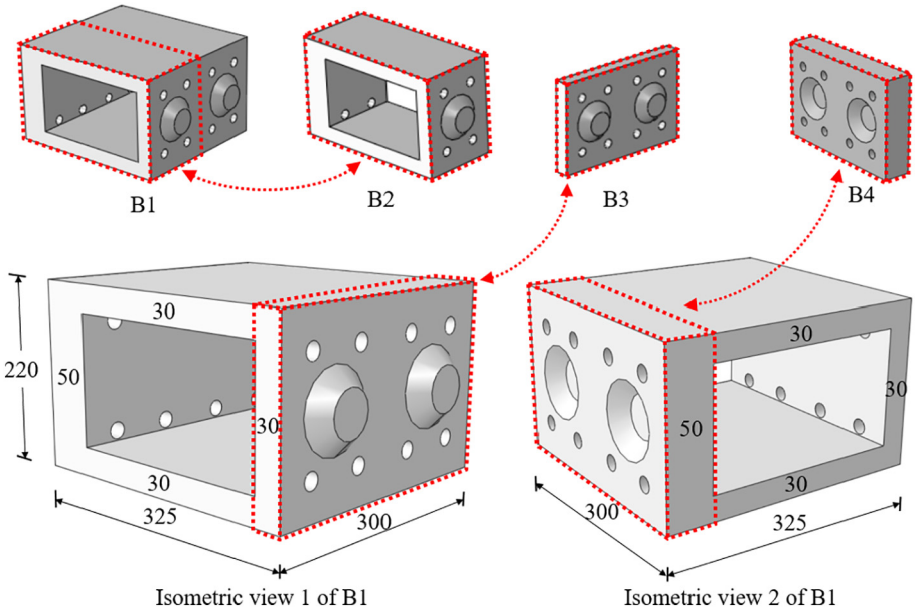

Fig. 3. Illustration of a set of four Lego-inspired blocks (RecoBlox™): (a) B1 (full block), (b) B2 (half block), (c) B3 (male plate), and (d) B4 (female plate). The blocks have shear keys and holes for passing bolts to joint multiple blocks. Dimensions are in mm.

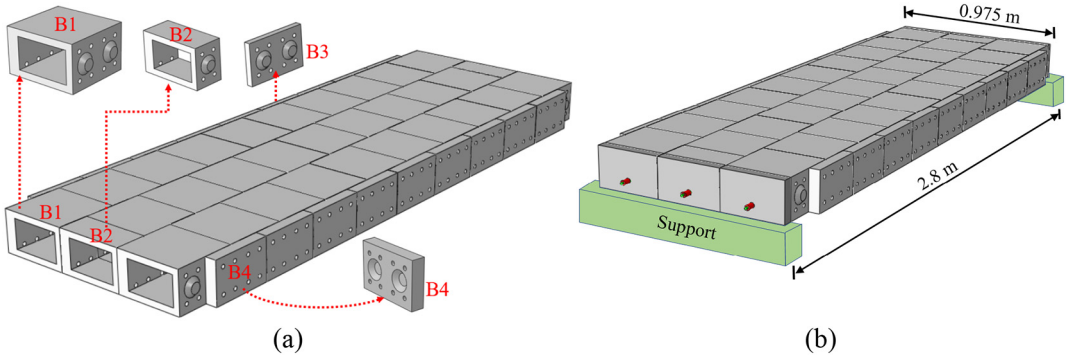

Fig. 4. Illustration of the footbridge assembled using Lego-inspired blocks: (a) before applying prestressing tendons, and (b) after applying prestressing tendons.

each set of bolt and washers (i.e. a steel bolt, two washers, and one lock washer), ensuring tight dry joints between the blocks and appropriate local stresses in the concrete near the bolts. The torque value was determined through a finite element analysis. In this feasibility study, the footbridge was supported by two rigid steel frames, which were used to simulate the bridge piers or abutments of real bridges.

Considering possible interference of the forces in different bolts on adjacent blocks, the bolting forces were monitored using a torque wrench to ensure that all the bolts were tight. After all the blocks were installed, three threaded bars were passed through the hollow section to apply prestressing forces, as indicated in Fig. 5. The tensile strength of the bars was 414 MPa. Each bar had a nominal diameter of 12.7 mm. At each end of the footbridge, three steel plates were used to anchor the three threaded bars on the blocks. The area of the steel plates fit the section of the blocks, and the plate thickness was 9.5 mm. The yielding strength of the steel was 345 MPa. The steel plates were in direct contact with the blocks at the two ends of the bridge. For passing and anchoring the threaded bars, each steel plate had a hole measuring 14 mm in diameter. There was a 25.4-mm distance between the hole and the centroid of the plate. The distance created an eccentricity of the prestressing forces in the bars. The eccentricity of the forces generates additional moment in the bridge, and in turn higher compressive stresses at the bottom and lower compressive stresses at the top of the bridge. This benefited the bridge subjected to the self-weight and pedestrian loads, because both the self-weight and pedestrian loads generated tensile stresses at the bottom and compressive stresses at the top of the bridge. With the eccentricity, the bridge's mid-span section was free of tensile stress under self-weight.

At each end of a threaded bar, a washer and two nuts were used to anchor the bar on the steel plates. Two nuts were used to effectively avoid possible slipping of the nuts during application of the prestressing forces. The prestress force in each threaded bar was applied using a wrench at one end of the bridge, namely the tensioning end; the other end of the bridge was namely the anchoring end. The force in each threaded bar was monitored using a load transducer installed at the anchoring end. The load cell was placed between the steel plate and a washer (see Fig. 5). The load cell had a force measurement capacity of 44.5 kN, and a manufacturer-specified nonlinearity of 0.25% of the rated output. The prestressing forces in the three threaded bars were applied through an iterative process until the force in each bar reached 10 kN. Finally, the footbridge was lifted using a crane and placed onto two rigid steel supports.

3.3. Experimental testing

Mechanical testing was conducted to evaluate the load-carrying performance of the footbridge. In addition to the load cells that measure the forces in the threaded bars, the deformations of the bridge were monitored using an optical tracking system, which used a camera to measure three-dimensional motions of multiple motion sensors

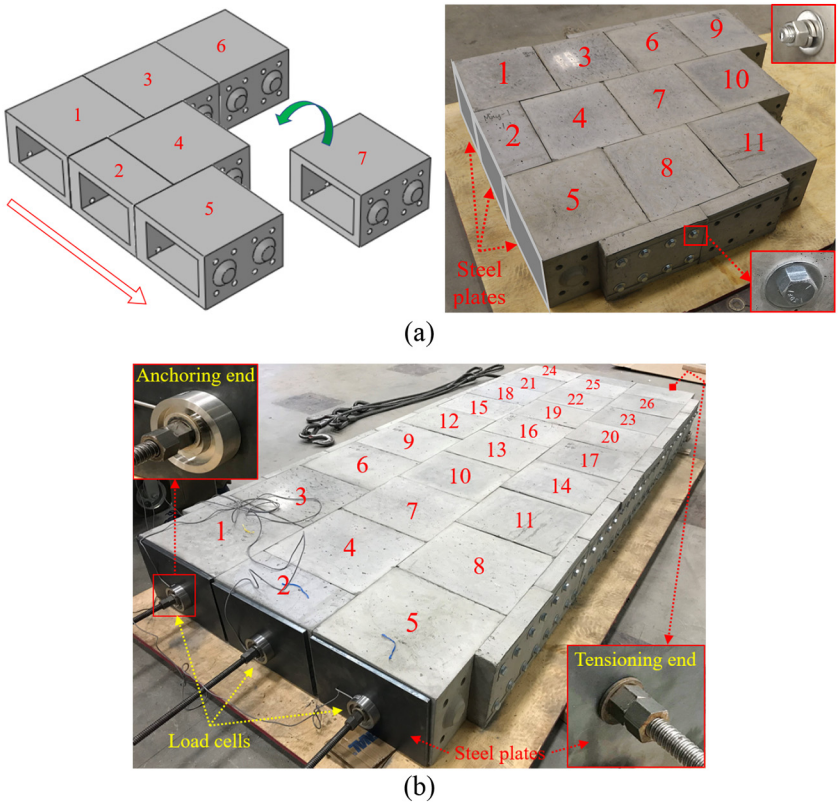

Fig. 5. Assembly of the blocks: (a) one step in the assembling process; (b) assembling sequence for the footbridge. The numbers in red color indicates the assembling sequence. (For interpretation of the references to color in this figure legend, the reader is referred to the web version of this article.)

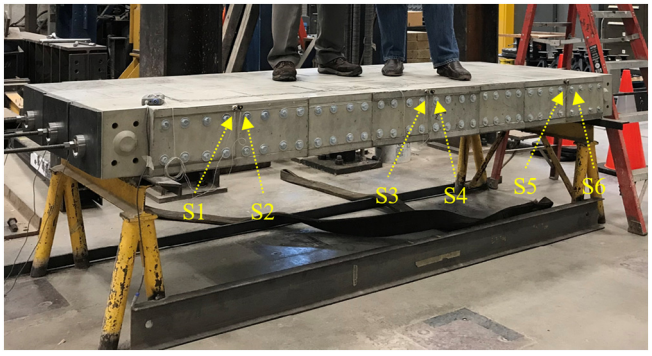

Fig. 6. Test set-up and instrumentation of the footbridge for mechanical loading tests. "S1" to "S6" represent six motion sensors for measuring the three-dimensional displacements.

attached on the surface of the bridge, as depicted in Fig. 6. Compared with the conventional displacement sensors, such as linear variable differential transformers, the optical tracking system provides non-contact displacement measurements in three dimensions with a measurement accuracy of 0.001 mm. This study used six motion sensors attached on the side surfaces of the bridge. The six sensors were designated as S1 to S6. The optical tracking system measured the three-dimensional deformations of the bridge at the three sections where the motions sensors were deployed.

After the bridge was erected, a 150-kg steel block was placed at the middle span of the bridge as a pre-load for examining the responses of the bridge under mechanical loading, before any pedestrian load was applied. According to the measurement from the motion sensors S3 and S4, the bridge's mid-span vertical deflection due to the placement of the steel block was < 1 mm, consistent with the prediction from the finite element analysis. According to the finite element analysis, as the applied mass is increased from 150 kg to 450 kg, the bridge does not have any damage, meaning that the bridge can carry the steel block with a dynamic factor of 3.0 (= 450 kg / 150 kg). Typically, the dynamic factor of moving load on a simply supported bridge is < 2.0. The pre-load test and the finite element analysis suggest that it is safe to conduct the pedestrian loading test. Finally, pedestrian loading was applied. In this feasibility study, the footbridge had enough deck area for two people walking on it at the same time. Thus, two adults walked through the bridge at normal walking speeds (~1.4 m/s). The total weight of the two adults was about 150 kg. The mid-span vertical deflection due to the pedestrian load was < 1/2000 of the span length. Throughout the testing, no crack due to the mechanical loading was observed. The bridge demonstrated reasonable load-carrying capability and stiffness.

After the above testing, the bridge was lifted and placed on the floor using the crane. Then, the bridge was disassembled following the sequence opposite to that in the assembling process. After disassemblage, the bridge's blocks were visually examined, with emphasis on the joints subjected to relatively high stresses in the assembling process and the mechanical testing. No visible crack was observed. Minor chipping was observed at a limited number of the edges and corners of the blocks, likely caused during the transportation of the blocks. The minor chipping was localized and did not affect the mechanical properties and functionality of the blocks.

4. Reconfigurability

4.1. Demonstration

To demonstrate the reconfigurability of the blocks, the blocks from the footbridge were reused to assemble a down-scaled frame, as shown in Fig. 7. The frame was composed of two columns and one beam, mimicking a part of a beam-column frame in a building. Compared with

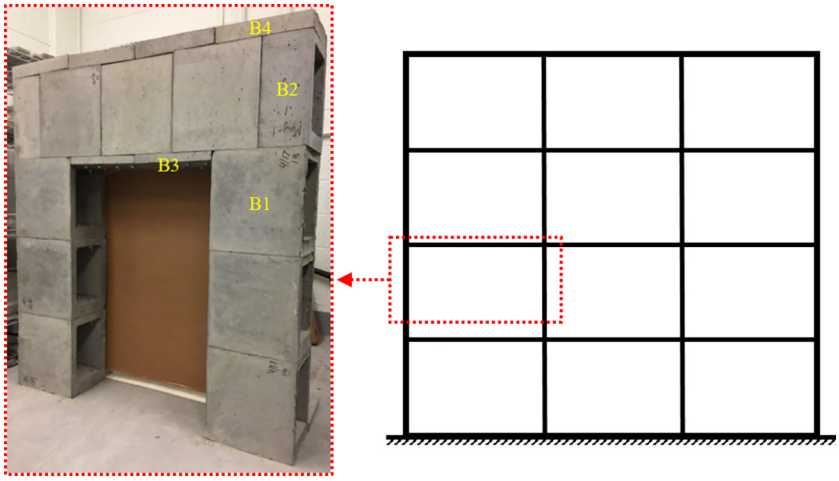

Fig. 7. Demonstration of reconfigurability: Reusing the blocks from the footbridge to assemble a part of a building frame.

the footbridge, the frame used the same blocks connected through the shear keys and steel bolts. More blocks can be added to the frame following the same assembling pattern to scale up the frame and form the main structure of the frame for a multi-story building. For the purpose of demonstration, the frame assembled using the blocks were only subjected to self-weight. No additional mechanical loading or prestressing force was applied in this study. In real applications, post-tensioned prestressing bars or tendons can be applied to enhance the load-carrying capacity if needed, depending on the structural analysis results. The application of post-tensioned bars can be similar to the bars used in the footbridge (Fig. 5). Further analysis on the reconfigured sections is presented in Section 4.2.

4.2. Comparative analysis

For further understanding of the performance of the reconfigured section, analysis is performed to compare the reconfigured section with a single-piece precast section fabricated in one cast. The reconfigured section uses the bendable concrete, while the single-piece section is made of conventional concrete. The compared characteristics include the load-carrying capacity, material costs, and production time. Fig. 8 depicts the locations and dimensions of the critical sections. In the analysis, reinforcement such as prestressed bar is not considered, consistent with the structure in Fig. 7. The mechanical analysis is conducted based on existing elastic/plastic analysis methods. The analysis process is elaborated in this sub-section.

Fig. 9 shows the strain and stress distributions over the depth of the cross sections. The compressive strength of the bendable concrete and conventional concrete is the same (46 MPa). For the tension behaviors of the bendable concrete, it is assumed that once the bendable concrete cracks, the tensile stress is equal to the first crack strength (4 MPa), so the strain-hardening effect is not considered, which is conservative. For the tension behaviors of the conventional concrete, once the concrete cracks, the concrete cannot carry more tensile force.

For S1 in Fig. 9(a), the compressive and tensile forces are in equilibrium, as expressed in Eq. (1):

$$0.85f_c' bc = f_t \times Area = f_t\,[b(325 + 50 - c) - (b - 30 - 30)(325 - 30 - 50)] \quad (1)$$

where f_c' and f_t are the compressive and tensile strengths of the bendable concrete, which are 46 MPa and 4 MPa, respectively; b is the width (220 mm) of the section; c is the compression depth (see Fig. 9).

Solving Eq. (1), c is determined:

$$c = 18.3\ mm \quad (2)$$

Given the uniform distribution of the tensile stress, the center of the tensile force is at the centroid of the area in tension, so the distance between the tensile force and the bottom fiber:

$$t = 184.2\ mm \quad (3)$$

Then, the moment capacity of the section S1 can be calculated:

$$M_{u1} = 0.85f_c' bc\left(325 + 50 - \frac{c}{2} - t\right) = 28.6\ kN{\bullet}m \quad (4)$$

The compressive strain at the top edge is:

$$\varepsilon_c = \frac{f_c'}{E} = \frac{46\ MPa}{23\ GPa} = 0.2\% \quad (5)$$

where E is the Young's modulus of the bendable concrete (E = 23 GPa).

According the plane cross section assumption, the tensile strain at the bottom edge is:

$$\varepsilon_t = \frac{\varepsilon_c}{c}(325 + 50 - c) = 3.8\% < 4\% \quad (6)$$

The maximum tensile strain is less than the tensile strain limit (4%, see Fig. 2). Therefore, it is reasonable to use the uniform distribution of the tensile stress in Fig. 9(a).

For S2 in Fig. 9(b), it is assumed that the maximum compressive stress (at the compression edge) in the bendable concrete does not reach its compressive strength. Then, the compressive and tensile forces are in equilibrium, as expressed in Eq. (7):

$$0.5\sigma_c bc = f_t \times Area = f_t\,[b(50 - c) + 30] \quad (7)$$

where σ_c is the compressive stress at the compression edge of the block.

Let the tensile strain at the tension edge reach the tensile strain limit (4%) of the bendable concrete, then,

$$\varepsilon_t = \frac{\sigma_c}{E}\left(\frac{325 + 30 + 50 - c}{c}\right) = 4\% \quad (8)$$

Solving Eqs. (7) and (8), σ_c and c are determined:

$$c = 14.9\ mm \quad (9a)$$

$$\sigma_c = 35.1\ MPa < 46\ MPa \quad (9b)$$

Eq. (9b) verifies the assumption that the maximum compressive stress in the bendable concrete does not reach its compressive strength.

Given the uniform distribution of the tensile stress, the center of the tensile force is at the centroid of the area in tension, so the distance between the tensile force and the bottom fiber:

$$t = 207.8\ mm \quad (10)$$

Then, the moment capacity of the section S2 can be calculated:

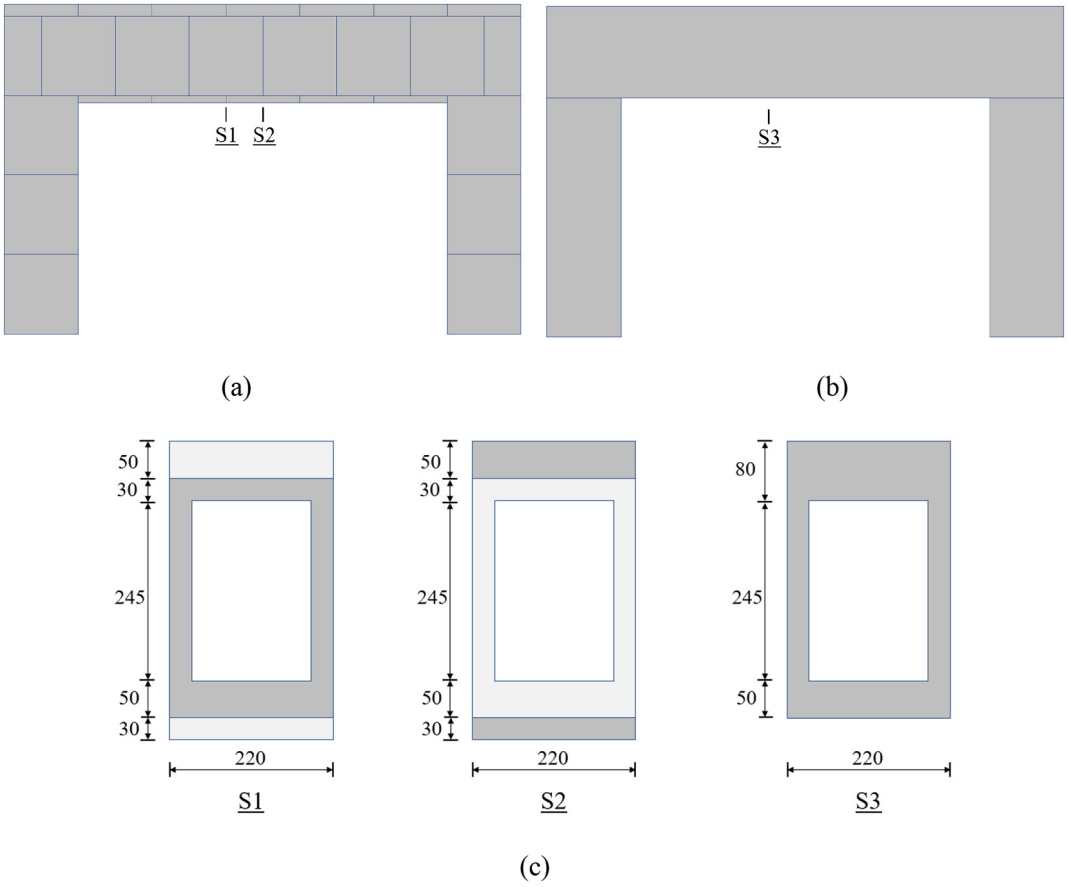

Fig. 8. Depiction of sections: (a) elevation view of reconfigured frame; (b) elevation view of precast beam and columns; (c) critical cross sections. Sections S1 and S2 are depicted in (a), and section S3 is depicted in (b). In S1 and S2 in (c), the area in the light color is discontinuous and thus not subjected to tension, as depicted in (a).

$$M_{u2} = 0.5\sigma_c bc\left(325 + 50 + 30 - \frac{c}{3} - t\right) = 25.1\ kN{\bullet}m \tag{11}$$

Since the value of M_{u2} is smaller than the value of M_{u1}, the section S2 dominates the load-carrying capacity of the reconfigured sections.

For S3 in Fig. 9(c), the compressive and tensile forces are in equilibrium, as expressed in Eq. (12):

$$0.5\sigma_c\left[bc - \frac{c-50}{c}(160)(c-50)\right] = 0.5f_t\left[bc - \frac{325-c}{375-c}(160)(325-c)\right] \tag{12}$$

Solving Eqs. (9a) and (9b), c is determined:

$$c = 200.0\ mm \tag{13}$$

Then, the moment capacity of the section S3 can be calculated:

$$M_{u3} = 0.5\sigma_c\left[bc - \frac{c-50}{c}(160)(c-50)\right](375)\left(\frac{2}{3}\right) = 7.4\ kN{\bullet}m \tag{14}$$

By comparing the values of M_{u2} and M_{u3}, without considering the strain-hardening effect of the bendable concrete, the load-carrying capacity of the reconfigured sections is 3.4 times that of the single-piece precast concrete section. In general, the unit material cost of the bendable concrete is about 3 times that of the conventional concrete with the same compressive strength. The ratio of capacity to material cost (i.e. capacity/cost) of the reconfigured section is comparable with the ratio of single-piece precast concrete section. In addition, recently, cost-effective versions of bendable concrete have been developed by using more cost-effective raw materials, such as supplementary cementitious materials, river sand, low-cost fibers, etc., further reducing the material cost of bendable concrete.

The sections (Fig. 9) without reinforcing bar have relatively low load-carrying capacities. To increase the load-carrying capacity, reinforcement can be applied. For the reconfigurable sections, post-tensioned bars can be employed in a manner similar to that in the footbridge (see Fig. 5). For single-piece precast components, either post-tensioned or pre-tensioned bars can be used, as well as embedded reinforcing bars in conventional reinforced concrete.

Regarding the construction time, compared with the single-piece precast section, the reconfigurable section needs additional time for the assembling operation. However, the single-piece precast section does not allow reconfiguration. Thus, once demolished, the precast components are either recycled after a series of processing or landfilled. This reflects the advantage of the configurable blocks. Further discussions on the construction efficiency, the design and manufacturing of the blocks are provided in the following section.

5. Discussions

5.1. Construction efficiency

In this feasibility study, the blocks were manually assembled and disassembled for the purpose of demonstration. With one person, the assembly operations of the footbridge took about 10 h, and the disassembly operations took about 4 h. More of the time was used to install or uninstall the bolts. The assembly operations took longer time than the disassembly operations, mainly because of the iterations in applying and checking the torque in each bolt. There was no need for such iterations in the disassembly process. For a bridge with the same overall dimensions and prefabricated as one part, the bridge can be cast as an

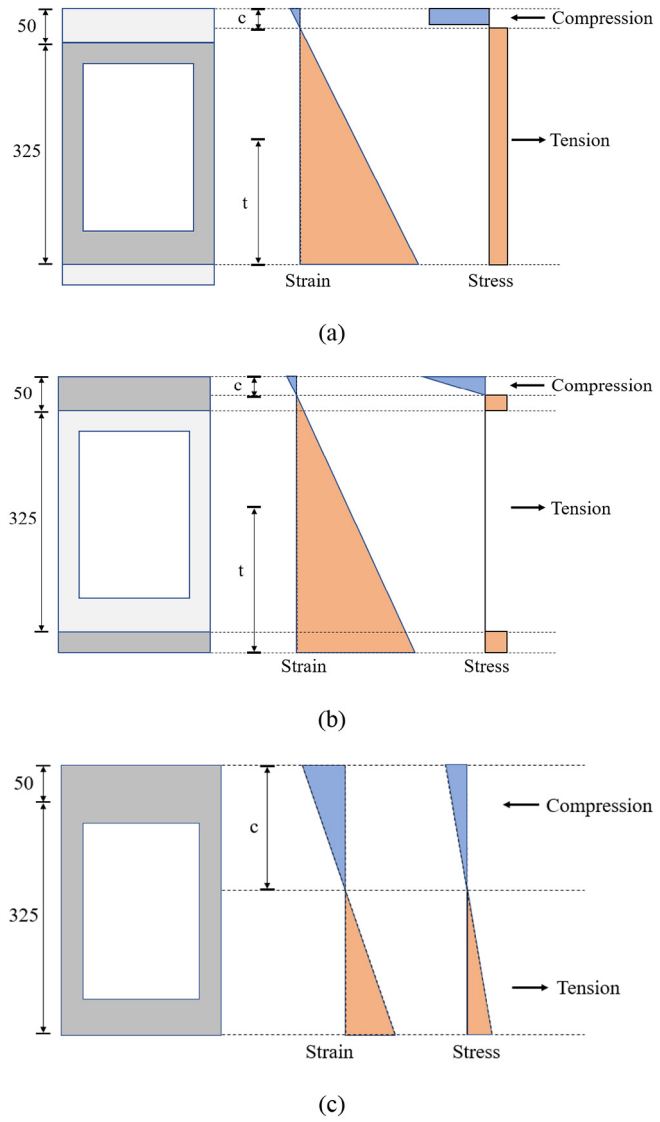

Fig. 9. Mechanical analysis of sections: (a) section S1, (b) section S2, and (c) section S3.

integrated part and placed by one lift, thus achieving higher efficiency than the presented construction method. However, the single-piece bridge is not available for reconfiguration.

In actual practice, to improve the construction efficiency, the assembling and disassembling operations (Fig. 5) will be performed using robotic systems. For the footbridge in this study, two robots can be used, one robot for placing the blocks and the other one for placing and tightening/loosening bolts. Placement of the blocks and installation of the bolts can be conducted by construction robots with high precision, as suggested in [32–34]. The robots can use computer vision-based techniques to locate objects with high precision [35], and use robotic arms to tighten or loosen the bolts [36]. The forces in the bolts can be measured by torque transducers in the robotic arm, and the measured bolt force can be used to control the robotic arms. With robots for installing or uninstalling the bolts, the construction efficiency will be greatly improved. According to prior practices of construction robots [32–34], it is envisioned that the assembly process of the footbridge will take < 1 h by using robotic systems in the future. When the RecoBlox™ are industrially scaled, the assembling time for a given structure will correspondingly be reduced.

5.2. Design of blocks

The preliminary design of the blocks (Fig. 3) is used to test the feasibility of the presented Lego-construction concept. The size of blocks was determined to be appropriate for manual operation by a single person. For industrial applications, the design of the blocks will be determined through an optimization process considering multiple aspects. First, the vision of the Lego-inspired construction is that a variety of structures can be assembled using limited types of standard blocks and a limited number of special blocks. Thus, multiple types of structures such as bridges and buildings will be considered to maximize the potential market and societal impacts of the innovation. Second, the design of the blocks must ensure appropriate mechanical performance of the assembled structures, such as the load-carrying capacity, seismic resistance, fatigue resistance, etc. Third, the blocks should be compatible with payload limits of robotic systems for digital construction. The blocks can be assembled and disassembled using construction robots for high construction efficiency and quality control.

This study shows that the presented blocks are feasible for construction of footbridge and certain components of buildings. The design of the blocks needs to be further optimized for wider applications in different types and sizes of structures, efficient use of materials, ease of fabrication and construction, maximized load-carrying capability, etc. In this study, steel bolts are used at the dry joints, which are subjected to corrosion. It is desired to conduct further research on other durable materials for the bolts, such as stainless steel and fiber reinforced polymers. The more durable materials might involve higher upfront cost, compared with conventional steel. However, the life-cycle cost may be lower, because the blocks and bolts can be reusable in different structures without the need of recycling. Also, the improved durability of the materials is expected to reduce the need of maintenance and rehabilitation, thus helping reduce the life-cycle cost.

5.3. Manufacturing of blocks

In this study, the blocks were fabricated through casting using customized molds. The molds led to additional cost of materials and time for fabricating the blocks, because of the needs to prepare the molds, demold, clean the molds, etc. Recent research suggested that three-dimensional printing (3DP) would be promising in manufacturing the blocks [37]. Bendable concrete mixtures have been tailored for 3DP with retained unique mechanical properties, crack resistance, and multifunctionality, as reported in [38,39]. With the current design of the blocks with sharp edges and corners, the printing efficiency may be limited, because the geometry requires either post-processing of printed blocks or incorporation of molds for shaping the edges and corners. For post-processing, a trowel-like shaping tool can be used in the printing, as demonstrated in Contour Crafting [40]. Also, it is possible to tailor the design of the blocks for 3DP. It is envisioned that 3DP will greatly enhance quality control and efficiency in manufacturing the blocks. Regarding the special blocks for specific structures, 3DP likely has more strengths, because of elimination or simplification of molding and demolding operations in 3DP. The designs of the block such as the geometry and dimensions will be adapted for 3DP and on-site assembly considerations, and the designs can be updated conveniently by modifying the computer models for 3DP.

6. Concluding remarks and future research

This paper presents a new paradigm of construction – Lego-inspired construction, and demonstrates its feasibility through a footbridge and frame assembled using RecoBlox™ blocks made of bendable concrete. Based on the investigations, the following conclusions can be drawn:

- The proposed concept of Lego-inspired construction is feasible for engineering structures such as the entire or parts of bridges and

buildings. The preliminary design of the blocks was verified by assembly of a prototype footbridge which showed reasonable load-carrying capability and stiffness to external mechanical loading. Under combined self-weight and pedestrian loading, the maximum deflection was < 1/2000 of the span length, and no visible crack was observed.

- With the dry joints, the structured assembled using the RecoBlox™ blocks can be disassembled, and the blocks can be used to assemble other structures with different configurations. In this study, disassembly of the footbridge was demonstrated following the sequence opposite to that in assembling the footbridge. After the disassembly, no visible damage was observed in the blocks. The blocks were reused to assemble a frame for buildings, demonstrating the reconfigurability of Lego-inspired construction.
- The proposed concept of Lego-inspired construction is promising to provide an alternative structural design and construction paradigm, which is possible to transform the current structural design and construction method. The new paradigm has great potential to improve the construction efficiency, productivity, safety, sustainability, and economic benefits in construction industry, as well as promoting digital manufacturing technologies such as large-scale 3D printing.

Despite the good promise, further research is needed before the proposed concept can be applied in real-life practices of construction. Some research needs are identified as follows:

- A systematic evaluation of the mechanical performance of assembled structures needs to be performed, such as the load-carrying capacity, seismic resistance, fatigue resistance, impact resistance, etc. The seismic resistance and fatigue resistance are particularly relevant in assembled structures using the proposed blocks, because the structures have more interfaces compared with the conventional cast-in-place structures or structures assembled using prefabricated components such as beams and columns.
- A thorough survey for potential applications of the proposed method is needed. While the proposed method may be applicable in multiple types of structures with different scales, it may be inappropriate for some types and sizes of structures, considering the reliability, economic benefits, sustainability, etc. Correspondingly, design optimization of the blocks should be performed for various applications in different scenarios. At the same time, potential social impacts should be considered as well in the survey to ensure acceptance of the public, in particular, provided the relatively conservative construction industry.
- Further research and development are needed for the manufacturing and construction processes. Three-dimensional printing techniques need to be improved to manufacture the blocks. Robotic systems for assembling and disassembling operations need to be designed and tested to enable the automation concept. In addition, to support the design, manufacturing, and construction aligned with the proposed method, condition assessment and quality control methods should be developed. In the meanwhile, corresponding technologies and standards must be developed towards commercialization.

Acknowledgement

This research was partially funded by the Clusters and Themes program and the MCubed 3.0 cross-disciplinary research program at the University of Michigan – Ann Arbor. Dr. He Zhu and Dr. Beata Jaworska helped cast the blocks. Dr. Kequan Yu help test the footbridge. Their contributions are gratefully acknowledged. Opinions, conclusions, and recommendations expressed in this paper are those of the authors and do not necessarily reflect those of the sponsors or the authors' affiliations.

References

[1] McKinsey Global Institute, Reinventing Construction Through a Productivity Revolution, February 2017, 2017. https://www.mckinsey.com/industries/capital-projects-and-infrastructure/our-insights/reinventing-construction-through-a-productivity-revolution.
[2] D. Randall, Construction Worker Shortage Weighs on Hot U.S. Housing Market, Reuters, Reuters.com, 2016.
[3] M. Marks, Construction: The Next Great Tech Transformation, Mckinsey.com, 2017.
[4] X. Li, Y. Zhu, Z. Zhang, An LCA-based environmental impact assessment model for construction processes, Build. Environ. 45 (3) (2010) 766–775, https://doi.org/10.1016/j.buildenv.2009.08.010.
[5] Federal Highway Administration, Prefabricated bridge elements and systems cost study: accelerated bridge construction success stories, https://www.fhwa.dot.gov/bridge/prefab/successstories/091104/01.cfm.
[6] M. Culmo, Accelerated bridge construction - experience in design, fabrication and erection of prefabricated bridge elements and systems, *Federal Highway Administration Rep-Ort (FHWA-HIF-12-013)*, Washington, D.C., United States, 2011 https://www.fhwa.dot.gov/bridge/abc/docs/abcmanual.pdf.
[7] M. Culmo, H. Boyle, S. Nettleton, V. Chandra, M. Tadros, J. Mallela, Engineering design, fabrication and erection of prefabricated bridge elements and systems, *Federal Highway Administration Report (FHWA-HIF-17-019)*, Washington, D.C., United States, 2013 https://www.fhwa.dot.gov/bridge/pubs/hif17019.pdf.
[8] N. Bertram, S. Fuchs, J. Mischke, R. Palter, G. Strube, J. Woetzel, Modular construction: from projects to products, McKinsey & Company Report, https://www.mckinsey.com/industries/capital-projects-and-infrastructure/our-insights/modular-construction-from-projects-to-products, (2019).
[9] Modular Building Institute, https://www.modular.org/HtmlPage.aspx?name=why_modular (Accessed on September 1, 2019).
[10] M. Culmo, Connection details for prefabricated bridge elements and systems, *Federal Highway Administration Report (FHWA-IF-09-010)*, Washington, D.C., United States, 2009 https://www.fhwa.dot.gov/bridge/prefab/if09010/report.pdf.
[11] U. S. Environmental Protection Agency, Advancing Sustainable Materials Management: 2015 Fact Sheet, https://www.epa.gov/sites/production/files/2018-07/documents/2015_smm_msw_factsheet_07242018_fnl_508_002.pdf, (2018) (Accessed on August 1, 2019).
[12] ASCE, Report Card for America's Infrastructure, https://www.infrastructurereportcard.org/cat-item/bridges/, (2017).
[13] U. S. Department of Transportation, Condition of U.S. highway bridges, https://www.bts.gov/content/condition-us-highway-bridges, (2018).
[14] H.J. Kong, S. Bike, V.C. Li, Development of a self-compacting engineered cementitious composite employing electrosteric dispersion/stabilization, Cem. Concr. Compos. 25 (3) (2003) 301–309, https://doi.org/10.1016/S0958-9465(02)00057-4.
[15] ASTM C109/C109M-16a, Standard Test Method for Compressive Strength of Hydraulic Cement Mortars (Using 2-in. or [50-mm] Cube Specimens), ASTM International, West Conshohocken, PA, 2016, www.astm.org. DOI:https://doi.org/10.1520/C0109_C0109M-16A.
[16] J.C. Committee, Recommendations for Design and Construction of High Performance Fiber Reinforced Cement Composites with Multiple Fine Cracks, Japan Society of Civil Engineers, Tokyo, Japan, 2008https://www.jsce.or.jp/committee/concrete/e/hpfrcc_JSCE.pdf.
[17] V.C. Li, On engineered Cementitious composites (ECC) - a review of the material and its applications, J. Adv. Concr. Technol. 1 (3) (2003) 215–230, https://doi.org/10.3151/jact.1.215.
[18] V.C. Li, S. Wang, C. Wu, Tensile strain-hardening behavior of polyvinyl alcohol engineered cementitious composite (PVA-ECC), ACI Mater. J. 98 (6) (2001) 483–492 https://www.concrete.org/publications/internationalconcreteabstractsportal/m/details/id/10851.
[19] Z. Zhang, S. Qian, H. Liu, V.C. Li, Ductile concrete material with self-healing capacity for jointless concrete pavement use, Transp. Res. Rec. 2640 (2017) 78–83, https://doi.org/10.3141/2640-09.
[20] V.C. Li, Engineered Cementitious Composites (ECC): Bendable Concrete for Sustainable and Resilient Infrastructure, Springer, 2019, https://doi.org/10.1007/978-3-662-58438-5.
[21] V.C. Li, T. Kanda, Innovations forum: engineered cementitious composites for structural applications, J. Mater. Civ. Eng. 10 (2) (1998) 66–69, https://doi.org/10.1061/(ASCE)0899-1561(1998)10:2(66).
[22] X. Li, Z. Xu, Y. Bao, Z. Cong, Post-fire seismic behavior of two-bay two-story frames with high-performance fiber-reinforced cementitious composite joints, Eng. Struct. 183 (2019) 150–159, https://doi.org/10.1016/j.engstruct.2019.01.015.
[23] X. Li, J. Wang, Y. Bao, G. Chen, Cyclic behavior of damaged reinforced concrete columns repaired with high-performance fiber-reinforced cementitious composite, Eng. Struct. 136 (2017) 26–35, https://doi.org/10.1016/j.engstruct.2017.01.015.
[24] E.H. Yang, V.C. Li, Tailoring engineered cementitious composites for impact resistance, Cem. Concr. Res. 42 (8) (2012) 1066–1071, https://doi.org/10.1016/j.cemconres.2012.04.006.
[25] S. Qian, V.C. Li, Headed anchor/engineered cementitious composites (ECC) pullout behavior, J. Adv. Concr. Technol. 9 (3) (2011) 339–351, https://doi.org/10.3151/jact.9.339.
[26] V.C. Li, High-performance and multifunctional cement-based composite material, Engineering 5 (2) (2019) 250–260, https://doi.org/10.1016/j.eng.2018.11.031.
[27] Y. Yang, M.D. Lepech, E.H. Yang, V.C. Li, Autogenous healing of engineered cementitious composites under wet-dry cycles, Cem. Concr. Res. 39 (5) (2009) 382–390, https://doi.org/10.1016/j.cemconres.2009.01.013.

[28] X. Li, Y. Bao, L. Wu, Q. Yan, H. Ma, G. Chen, H. Zhang, Thermal and mechanical properties of high-performance fiber-reinforced cementitious composites after exposure to high temperatures, Constr. Build. Mater. 157 (2017) 829–838, https://doi.org/10.1016/j.conbuildmat.2017.09.125.
[29] R. Ranade, J. Zhang, J.P. Lynch, V.C. Li, Influence of micro-cracking on the composite resistivity of engineered cementitious composites, Cem. Concr. Res. 58 (2014) 1–12, https://doi.org/10.1016/j.cemconres.2014.01.002.
[30] M. Xu, Y. Bao, J. Yu, K. Wu, H. Shi, X. Guo, V.C. Li, Multiscale investigation of tensile properties of a TiO_2-doped engineered Cementitious composite, Constr. Build. Mater. 209 (2019) 485–491, https://doi.org/10.1016/j.conbuildmat.2019.03.112.
[31] Y. Bao, Y. Chen, M.S. Hoehler, C.M. Smith, M. Bundy, G. Chen, Experimental analysis of steel beams subjected to fire enhanced by Brillouin scattering-based fiber optic sensor data, J. Struct. Eng. 143 (1) (2016) 04016143, , https://doi.org/10.1061/(ASCE)ST.1943-541X.0001617.
[32] CNBC website, https://www.cnbc.com/video/2018/02/17/construction-robotics-bricklaying-robots-build-home.html (Accessed on September 1, 2019).
[33] Introduction to construction robotics and the bricklaying robot SAM. https://www.youtube.com/watch?v=bDRCWnsFnC4. Accessed on September 1, 2019.
[34] Construction Robotics Bricklaying Robot SAM100, https://www.youtube.com/watch?v=mP2AtqcitbQ (Accessed on September 1, 2019).
[35] C.J. Liang, K.M. Lundeen, W. McGee, C.C. Menassa, S. Lee, V.R. Kamat, A vision-based marker-less pose estimation system for articulated construction robots, Autom. Constr. 104 (2019) 80–94, https://doi.org/10.1016/j.autcon.2019.04.004.
[36] Assembly. Robots for flexible torqueing. https://www.assemblymag.com/articles/83341-robots-for-flexible-torquing. Accessed on September 1, 2019.
[37] Y.W.D. Tay, B. Panda, S.C. Paul, N.A. Noor Mohamed, M.J. Tan, K.F. Leong, 3D printing trends in building and construction industry: a review, Virtual and Physical Prototyping 12 (3) (2017) 261–276, https://doi.org/10.1080/17452759.2017.1326724.
[38] D.G. Soltan, V.C. Li, A self-reinforced cementitious composite for building-scale 3D printing, Cem. Concr. Compos. 90 (2018) 1–13, https://doi.org/10.1016/j.cemconcomp.2018.03.017.
[39] Y. Bao, M. Xu, D. Stolen, V.C. Li, Three-dimensional printing self-cleaning engineered cementitious composites for structural elements, 1st International Conference on Concrete and Digital Fabrication, Digital Concrete 2018 – Zurich, Switzerland, 10–12 September, 2018, 2018, https://doi.org/10.1007/978-3-319-99519-9_11.
[40] B. Khoshnevis, D. Hwang, K. Yao, Z. Yeh, Mega-scale fabrication by contour crafting, Int. J. Ind. Syst. Eng. 1 (3) (2006) 301–320, https://doi.org/10.1504/IJISE.2006.009791.